ELSEVIER

Earth and Planetary Science Letters 170 (1999) 181–196

EPSL

www.elsevier.com/locate/epsl

The correlation between $^{18}O/^{16}O$ ratios of meteoric water and surface temperature: its use in investigating terrestrial climate change over geologic time

Henry C. Fricke *, James R. O'Neil

Department of Geological Sciences, University of Michigan, Ann Arbor, MI 48109-1063, USA

Received 12 June 1998; revised version received 24 March 1999; accepted 6 April 1999

Abstract

Correlations between mean annual temperature (MAT) and the weighted average oxygen isotope composition of yearly precipitation ($\delta^{18}O_{pt}$) are well-known, but the utility of modern relations to make reliable estimates of temperature change over geological time is uncertain. This question has been addressed by using seasonal subsets of the global data base of temperature and isotopic measurements to represent two different climate modes. A comparison of middle- to high-latitude $\delta^{18}O_{pt}$/temperature relations for each climate mode reveals (1) a significant offset between them, and (2) a difference in the strength of their correlations. The offset in relations is due to differences in temperature and water vapor budget in the tropics, and can lead to serious underestimates of temperature change. Differences in the strength of correlations arise from the influence of climate mode-specific, non-temperature factors on $\delta^{18}O_{pt}$. The overall result is that no single relation can be used in all cases to make unambiguous temperature estimates using a temporal record of $\delta^{18}O_{pt}$ values. One way to overcome these problems is to reconstruct $\delta^{18}O_{pt}$/temperature relations for the time periods being investigated. If an appropriate proxy for $\delta^{18}O_{pt}$ is available, it may also be possible to estimate temperature *without* relying on $\delta^{18}O_{pt}$/temperature relations. A promising alternative to these options is to use records of $\delta^{18}O_{pt}$ to test predictions of global climate models, an approach that may allow a reliable and more complete reconstruction to be made of climate change over geologic time. © 1999 Elsevier Science B.V. All rights reserved.

Keywords: O-18/O-16; meteoric water; isotope ratios; seasonal variations; paleoclimatology; climate; paleotemperature

1. Introduction

Over the last several decades, investigation of the stable isotope systematics of precipitation has added a great deal to our understanding of the source and transport of moisture in the atmosphere. One of the most important contributions resulting from this research was the identification of a good correlation between mean annual surface temperature and the weighted oxygen isotope composition of precipitation ($\delta^{18}O_{pt}$) at mid- to high-latitude regions, whereby higher temperatures correspond to higher $\delta^{18}O_{pt}$ values [1–3]. Although this relation is not perfectly understood, it is generally agreed that $\delta^{18}O_{pt}$/temperature covariance is consistent with continual lowering of $^{18}O/^{16}O$ of vapor in the air mass due

* Corresponding author. Present address: Geophysical Laboratory, Carnegie Institution of Washington, Washington, DC 20015, USA. Fax: +1 202 686 2410; E-mail: fricke@gl.ciw.edu

0012-821X/99/$ – see front matter © 1999 Elsevier Science B.V. All rights reserved.
PII: S0012-821X(99)00105-3

to preferential incorporation of ^{18}O into condensate during adiabatic processes of cooling [1–5]. The air masses lose water as they move along surface temperature gradients from tropical to polar latitudes, inland from the sea, or to higher elevations. It should be stressed that, while the temperature of the air mass controls condensation, it is exchange between condensate and water vapor at the warmer temperatures of the cloud base that provides the most reasonable physical basis for the relation between surface temperature and $\delta^{18}O_{pt}$ values [5].

In contrast to phenomena occurring at higher latitudes, there is no correlation between surface temperature and $\delta^{18}O$ values of precipitation in the tropics [1–3]. Tropical regions are characterized by converging air masses that are forced to move vertically rather than horizontally. As a result they are cooled predominately by convection in atmospheric towers, while surface temperature gradients remain negligible. Although temperature does not correlate with $\delta^{18}O_{pt}$ in the tropics, a negative correlation has been observed between the amount of rainfall and $\delta^{18}O_{pt}$ values at tropical island locations, and is termed the *amount effect* [1]. It is caused by gradual saturation of air below the cloud base as precipitation proceeds, an effect that diminishes any shift to higher $\delta^{18}O_{pt}$ values caused by evaporation during precipitation [1], and by the preferential loss of ^{18}O from an air mass as rainout continues.

The oxygen isotope composition of past precipitation can be measured directly on ice cores, ground waters, fluid inclusions, or estimated by measuring the oxygen isotope ratio of a proxy material such as skeletal remains of animals, lake sediments, and soil minerals that formed in equilibrium with surface or ground waters. Because other kinds of geochemical climate records are lacking for terrestrial environments, the $\delta^{18}O_{pt}$/temperature relation for middle- to high-latitude precipitation has garnered a great deal of attention as a possible tool for investigating terrestrial climatic conditions from the Mesozoic to the present [6]. Nevertheless, it remains difficult to make quantitative climatic interpretations of a temporal record of $\delta^{18}O_{pt}$ values. Factors other than temperature are affected by climate change, and they too can have a local influence on how $\delta^{18}O_{pt}$ changes over time. For example, during the Holocene–glacial transition, a change in the position of boundaries between air masses played a predominant role in determining $\delta^{18}O_{pt}$ at some high latitude locations [7,8]. Even if it *could* be ascertained that temperature was the underlying cause of variations in $\delta^{18}O_{pt}$ over time in a given location, many observations lead to the conclusion that the present-day relation between temperature and $\delta^{18}O_{pt}$ may not be the appropriate one to use in estimating temperature change over time [9–13].

The goal of this paper is to consider those problems associated with the $\delta^{18}O_{pt}$ paleothermometer from the perspective of global changes in climate, and to discuss ways to overcome them. The global perspective is provided by using seasonal subsets of isotopic and temperature data from a global network of collection stations to represent the conditions that prevail under fundamentally different global climate modes. Although changes in season are not completely analogous to longer-term changes in climate mode, the stable isotope systematics of summer and winter precipitation are well documented and provide a simple model for identifying understanding which factors influence the relation between $\delta^{18}O_{pt}$ and temperature thus allowing a more sensible interpretation to be made of $\delta^{18}O_{pt}$ data. An analysis of the seasonal data indicates that it should be possible to use records of $\delta^{18}O_{pt}$ from proxy data as a quantitative paleothermometer over geologic time by reconstructing $\delta^{18}O_{pt}$/temperature relations in that region for time periods in the past. In addition to their potential as a paleothermometer, records of $\delta^{18}O_{pt}$ may also prove ideal for testing predictions of climate change made using global climate models.

2. Methods

Monthly averages of temperature and $\delta^{18}O_{pt}$ from the global network of weather stations operated by the IAEA–WMO (International Atomic Energy Agency–World Meteorological Organization) [14] are grouped by season to create average values at each locality for summer and winter (Table 1). Values for each season are then compared in order to determine the nature of global patterns in temperature and $\delta^{18}O_{pt}$ under climate conditions, or modes, that are distinctly warmer and cooler than the mean annual conditions that exist at present. Patterns con-

Table 1
Summer and winter averages for global climate and isotope data

Station	Latitude (°)	Winter oxygen ($\delta^{18}O$)	Summer oxygen ($\delta^{18}O$)	Winter temperature (°C)	Summer temperature (°C)
Tropics					
Addis Abada	9	0.39	−1.22	15.58	15.87
Alice Springs*	23.8	−3.71	−4.41	12.21	27.87
Asuncion*	25.27	−3.5	−6.3	19.4	28.7
Bamako	12.63	no rain	−4.58	25.75	27.5
Bangkok	13.73	−2.06	−5.51	26.63	28.63
Barbados Is.	13.07	0.8	−1.82	25.57	27.28
Barranquilla	10.88	−5.2	−4.08	26.53	27.93
Belem*	1.43	−0.77	−2.16	25.89	25.8
Bogata	4.7	−4.95	−10.57	12.88	13.14
Bombay	18.9	−0.2	−1.23	25.1	28
Brasilia*	15.85	−1.78	−5.15	19.1	21.65
Cayenne	4.83	−1.14	−3.83	25.17	25.25
Ceara Minim*	5.8	−1.34	−1.23	24.45	26.28
Corrientes*	24.47	−3.51	−7.84	15.66	25.85
Culaba*	15.6	−5.87	−0.89	24.1	26.7
Dar es Salaam*	6.88	−1.21	−2.16	23.82	27.33
Darwin*	12.43	−2	−4.51	25.68	28.87
Djajpura*	2.53	−4.93	−5.5	25.17	27.07
Djakarta*	6.18	−4.62	−5.93	26.8	26.58
Entebbe	0.05	−1.57	−2.37	20.85	21.95
Fortaleza*	3.72	−1.82	−1.57	25.59	26.99
Geneina	13.48	no rain	−1.41	22.71	27.4
Guilin	25.21	−8.2	−2.9	9	27.8
Hong Kong	22.32	−2.45	−7.02	16.15	25.01
Howard AFB	8.92	−1.12	−5.94	27.06	27.07
Izobamba*	0.37	−11.39	−8.83	10.93	11.21
Jedda	21.3	−1.28	no rain	24.14	30.78
Kano	12.05	no rain	−3.56	22.38	26.72
Karachi	24.9	−0.83	−3.44	17.87	29.36
Khartoum	15.6	no rain	−1.44	23.22	31.82
Kinshasa*	4.37	−2.03	−3.42	22.3	24.73
Kuming	25.05	−11.7	−3.92	19.7	8.9
Ko Samui	9.28	−3.35	−3.39	26.83	28.28
Ko Sichang	13.17	−5.25	−5.27	26.59	29.97
Luang P.	19.88	−3.1	−7.48	21.64	28.01
Madung*	5.22	−5.04	−8.76	26.78	26.25
Malange	9.55	−0.67	−4.65	22.85	22.34
Manaus*	3.12	−2.82	−4.19	26.9	26.35
Manila	14.52	−3.11	−6.18	25.3	27.5
Maracay	10.25	−2.13	−3.54	23.52	24.47
Menongue*	14.67	0.21	−6.34	16.65	21.26
Muguga*	1.22	−1.53	−2.54	n.m.	n.m.
N'djamen	12.13	no rain	−2.56	24.28	27.7
Ndola*	13	no rain	−6.59	18.09	22.67
P. Velho*	8.77	−3.72	−6.82	24.7	25.4
Pretoria*	25.73	−0.55	−3.53	12.25	21.94
Rio D.*	22.9	−2.58	−4.76	21.57	26.13
Salvador*	13	−1.54	−0.89	23.76	26.23
Salta*	24.78	−2.03	−5.64	11.11	18.47
San Gabriel	0.13	−2.77	−3.87	25.87	24.83
San Juan Is.	18.43	−1.05	−1.57	25.42	28.17

Table 1 (continued)

Station	Latitude (°)	Winter oxygen ($\delta^{18}O$)	Summer oxygen ($\delta^{18}O$)	Winter temperature (°C)	Summer temperature (°C)
San Salvador	13.7	−3.44	−6.47	22.27	23.88
Shillong	25.57	−1.71	−5.93	12.25	21
Singapore	1.35	−6.21	−6.76	25.6	26.63
Ushulala*	54.78	−12.07	−10.11	2.2	9.68
Veracruz	19.2	−0.61	−3.97	21.86	28.22
Windhoek*	22.57	−1.15	−4.02	14.25	22.99
Yap Is.	9.49	−3.41	−6.4	26.84	27.07
Middle latitudes					
Adana	36.98	−6.21	−2.75	10.44	26.91
Adelaide*	34.93	−4.83	−3.74	12.06	21.9
Alexandria	31.2	−4.23	no rain	9.01	25.38
Amman, Jor.	31.98	−5.75	no rain	n.m.	n.m.
Ankara	39.95	−11.12	−4.13	1.2	21.65
Antanan*	36.88	−3.18	−8.53	14.41	20.2
Antalya	36.88	−6.08	−3.9	10.34	27.12
Astrakhan	46.25	−11.6	−5.85	−3.17	27.22
Athens	37.9	−6.96	−2.67	10.49	25.43
Atikokan	48.75	−22.79	−9.53	−16.44	15.8
Barcelona	41.38	−6.21	−3.06	9.69	22.37
Bahrain	26.27	−0.05	no rain	17.92	33.5
Batumi	41.39	−10.19	−6.56	8.03	22.4
Beer Shava	31.15	−5.63	no rain	12.46	25.47
Beja, Port.	38.01	−5.94	−4.19	10.64	23.68
Berlin	52.07	−10.6	−7.03	0.68	17.39
Bern	46.92	−12.66	−7.12	0.32	17.26
Bet Dagan	32	−5.1	no rain	13.06	25.57
Brest	52.07	−13.66	−7.23	−2.04	17.3
Brisbane*	27.43	−4.12	−3.42	16.22	24.95
Buenos Aires*	34.58	−4.35	−3.09	11.06	23.33
Cape Grim*	40.68	−5.07	−2.78	10.28	15.11
Changsha	28.1	−4.63	−8.03	6.32	28.3
Chicago	41.78	−12.34	−3.09	−3.64	22.63
Chihuahau	28.63	−9.25	−5.6	10.42	24.97
Coshocton	40.37	−11.4	−4.7	n.m.	n.m.
Crete	35.2	−6.83	no rain	13.28	30.6
Edmonton	53.57	−27.06	−13.85	−12.12	16.47
Faro	37.01	−4.87	−1.57	12.85	22.85
Flagstaff	35.13	−10.93	−3.63	−1.21	16.75
Fuzhou	26.09	−4.75	−6.85	12.53	28.92
Genoa	44.42	−6.16	−3.73	7.6	21.29
Gibralter	36.15	−4.62	−2.17	13.6	22.98
Gimli	50.62	−24.81	−10.24	−16	18.08
Goose Bay	53.32	−19.91	−12.45	−13.47	13.5
Gorki	56.13	−15.68	−9.31	−8.2	17.44
Grimsel	46.57	−16.83	−10.3	−5.04	8.42
Groningen	53.21	−9.1	−6.3	2.65	16.56
Guiyang	26.35	−4.26	−9.5	5.5	24.59
Guttane, Swit.	46.65	−16.03	−8.6	−1	14.25
Har Kanan	32.97	−6.83	no rain	8.85	23.73
Hatteras	35.07	−4.84	−3.49	7.98	24.84
Kabul	34.67	−10.57	−1.12	−0.56	22.92
Kalinin	56.54	−16.76	−8.38	−7.81	16.4

Table 1 (continued)

Station	Latitude (º)	Winter oxygen ($\delta^{18}O$)	Summer oxygen ($\delta^{18}O$)	Winter temperature (ºC)	Summer temperature (ºC)
Kataia*	35.07	−5.36	−3.64	12	18.76
Keyworth	52.52	−8.7	−5.6	7.61	20.63
Kirov	58.39	−16.77	−9.91	−10.83	16.79
Konstanz	47.68	−12.78	−6.98	0.72	17.8
Krakow	50.07	−12.92	−7.15	−1.38	17.07
L'vov	49.49	−14.05	−7.77	−2.33	16.54
La Suela*	30.58	−5.5	−4.76	12.15	23.63
Leige	50.7	−8.73	−5.05	n.m.	n.m.
Lista	58.1	−7.55	−5.35	1.12	13.68
Ljubljana	46.04	−11.67	−6.9	0.17	19.29
Loncarno, Swit.	46.17	−12.17	−5.9	3.86	20.1
Malan*	33.97	−3.57	−1.92	12.05	20.05
Meiringe, Swit.	46.73	−15.24	−7.83	0.19	15.7
Melbourne*	37.82	−5.66	−4.16	10.52	20.08
Mendoza*	32.88	−10.8	−3.5	8.2	23.8
Minsk	52.52	−14.46	−8.81	−5.21	19
Moskova	55.75	−16.3	−7.69	−7.37	17.92
Najing	32.05	−7.4	−9.64	2.86	26.39
Nanuncun*	34.03	−9.8	−3.69	6.95	22.37
New Dehli	28.58	−0.87	−3.83	15.59	31.37
Odessa	46.48	−11.91	−6.76	−0.31	19.89
Ottawa	45.32	−16.91	−7.83	−9.05	19.35
Perm	58.01	−18.23	−3.53	−12.11	16.4
Perth*	31.95	−3.97	−1.79	13.96	23.83
Petzenkirchen	48.15	−13.63	−6.39	0.08	17.43
Pohang	36.03	−6.13	−8.47	1.99	23.51
Porta, Port.	41.09	−6.25	−4.04	9.29	23.11
Porto Alegre*	30.08	−4.17	−5.29	14.83	24.11
Puerto Monte*	41.47	−6.88	−5.17	6.62	13.8
Quiqihar	47.23	−23.77	−9.51	−15.9	21.19
Rhodes	36.38	−4.97	no rain	11.15	26.1
Riga	56.97	−11.45	−8	−4.44	15.77
Rjazan	54.37	−15.1	−7.2	−7.66	18.27
Rostov	47.25	−11.42	−4.97	−2.88	20.93
Ryori	39.02	−9.2	−8.2	0.33	18.94
Sant. del. Sst*	27.78	−2.9	−5.07	12.28	25.91
Santiago*	33.45	−8.73	no rain	8.78	21.25
Saratov	51.34	−15.39	−7.26	−7.54	21.31
Shijiazuang	38.02	−11.21	−7.53	−0.74	25.77
Sidi Barani	31.63	−5.76	no rain	19.67	24.69
Simcoe	42.85	−15.72	−6.35	−5.31	20.26
St. Agathe	46.05	−13.7	−8.11	−11.57	19.23
St. Petersburg	59.58	−13.94	−10.01	−5.84	16.4
Stuttgart	48.83	−10.77	−5.87	1.25	17.72
Taastrap	55.67	−11.15	−7.49	n.m.	n.m.
Teheran	35.68	−6.49	−1.57	4.66	28.04
The Pas	53.97	−26.14	−13.41	−17.78	16.74
Thonon-Bains	46.22	−11.87	−6.41	2.46	18.9
Tianjin	39.55	−11.78	−7.66	−0.58	27.93
Tokyo	35.68	−8.46	−6.98	6.04	24.72
Truro	45.37	−12.66	−7.02	−4.7	17.58
Tunis	36.83	−5.01	1.39	11.85	26.39
Ulan Bator	47.45	−14.83	−7.48	−17.9	15.66

Table 1 (continued)

Station	Latitude (°)	Winter oxygen ($\delta^{18}O$)	Summer oxygen ($\delta^{18}O$)	Winter temperature (°C)	Summer temperature (°C)
Valentia	51.93	−8.9	−5.76	7.05	14.47
Victoria	48.25	−10.89	−8.51	4.97	16.42
Vienna	48.64	−13.65	−6.68	0.57	19.17
Volgada	59.17	−17.56	−9.69	−10.72	15.39
Waco	31.62	−6.39	−2.03	8.88	29
Wallingford	51.37	−8.12	−5.21	7.34	21.08
Wirzburg	49.8	−9.97	−6.29	0.81	17.56
Wynard	51.77	−25.85	−13	−14.08	15.15
Xian	34.3	−7.64	−5.75	1.47	25.16
Yinchuan	38.3	−15.51	−6.32	−5.53	22.2
Zagreb	45.49	−11.88	−6.28	1.87	22.01
Polar latitudes					
Amderma	69.46	−19.54	−11.91	−18.63	5.1
Archanglsk	64.58	−18.61	−9.44	−12.09	14.3
Barrow	71.3	−21.41	−13.72	−25.94	2.35
Bethel	60.78	−14.81	−10.36	−14.3	11.36
Ft. Smith	60.02	−25.92	−15.06	−23.48	14.78
Groennedal	61.22	−13.22	−11.39	−4.26	7.29
Halley Bay*	75.5	−26.09	−14.58	−27.65	−6.15
Isfjord	78.07	−10.39	−8.28	−11.78	3.51
Murmansk	68.58	−15.73	−3.45	−10.61	11.38
Nord	81.6	−29.64	−17.22	−29.93	1.2
Pechora	65.07	−20.37	−10.94	−17.14	13.48
Prins Christian	60.02	−12.56	−9.72	−3.81	5.99
Reykjavik	64.13	−8.1	−7.6	0.1	10
Scoresbury	70.5	−15.67	−10.01	−15.6	1.7
Thule	76.52	−30.37	−18.87	−23.67	3.06
Whitehorse	60.72	−22.64	−18.02	−15.42	12.77

Temperature and $\delta^{18}O_{pt}$ for summer and winter seasons for all IAEA weather stations with at least three years of isotopic data [10]. The mean monthly data for December, January, and February are averaged to represent winters in the northern hemisphere and summers in the southern hemisphere, while data for June, July, and August represent the opposite season. A single asterisk '*' indicates that a given locality is located in the southern hemisphere. The weather stations are also separated spatially into tropical, middle latitude, and polar zones with approximate boundaries at 25° and 60° latitude.

structed in this way may not accurately represent conditions prevailing during periods in the past when *mean annual* climate was different, but they do provide a heretofore unavailable means of investigating the effects of global changes in temperature and insolation in an empirical rather than theoretical manner.

All IAEA–WMO stations with at least three years of $\delta^{18}O_{pt}$ data are included in this study. Including shorter records greatly increases the geographic area represented by the data set, but also increases the possibility that these records are inappropriate because of the inclusion of years with anomalous temperature and $\delta^{18}O_{pt}$. The months of June, July, and August are defined as *summer* in the northern hemisphere and *winter* in the southern hemisphere, while December, January, and February define *winter* in the northern hemisphere and *summer* in the southern hemisphere. These months were chosen to facilitate comparison with previous work on seasonal differences in temperature and $\delta^{18}O_{pt}$ values [11,15], and to isolate seasonal extremes in climate variables and $\delta^{18}O_{pt}$ values from the generally 'transitional' seasons of spring and fall. Seasonal extremes, however, may not coincide exactly with these months at all localities. Near the equator in particular, the position of the boundary between northern and southern hemisphere air masses (intertropical convergence zone) is highly variable, so designating the months

of June, July and August as winter or summer may not be as meaningful for stations at low latitude.

The IAEA–WMO stations have also been assigned to groups defined by ranges of latitude in an effort to isolate isotopic and temperature differences between tropical, middle-latitude, and polar air masses. It should be noted that air mass boundaries are by nature diffuse and variable in position, so there may be regional differences in circulation patterns that cannot be distinguished. Nevertheless, as a first-order approximation, 25° latitude will be considered the boundary between tropical and mid-latitude air masses, and 60° latitude will be considered the boundary between mid-latitude and polar air masses. These latitudes roughly correspond to the bands of high and low atmospheric pressure, respectively, that characterize the three Hadley cells associated with idealized atmospheric circulation.

3. Results

Once the IAEA–WMO data are assigned to different climate modes and latitudinal bands, they can be plotted in a number of ways. Of interest for this study are latitudinal gradients in temperature and $\delta^{18}O_{pt}$ under summer and winter climate modes, and the resulting $\delta^{18}O_{pt}$/temperature relations. Latitudinal temperature gradients are illustrated in Fig. 1. As expected, summer temperatures are always higher than winter temperatures, but the *magnitude* of this difference (seasonality) increases with latitude because high latitude regions undergo more extensive heating and cooling in response to seasonal changes in insolation than do the tropics. The result is that the latitudinal temperature gradient for summer conditions of ~0.22°C/° latitude is about half the ~0.44°C/° latitude range observed for winter conditions. Another important feature of Fig. 1 is the dependence of the temperature/latitude relation on geographic location. Temperatures vary irregularly in the tropics whereas, at higher latitudes, there is a systematic decrease in temperature with latitude.

It is evident from Fig. 2 that trends in $\delta^{18}O_{pt}$ with latitude are similar to those with temperature. There is no systematic variation of $\delta^{18}O_{pt}$ values in the tropics while at higher latitudes $\delta^{18}O_{pt}$ decreases regularly with distance from the equator. In addition,

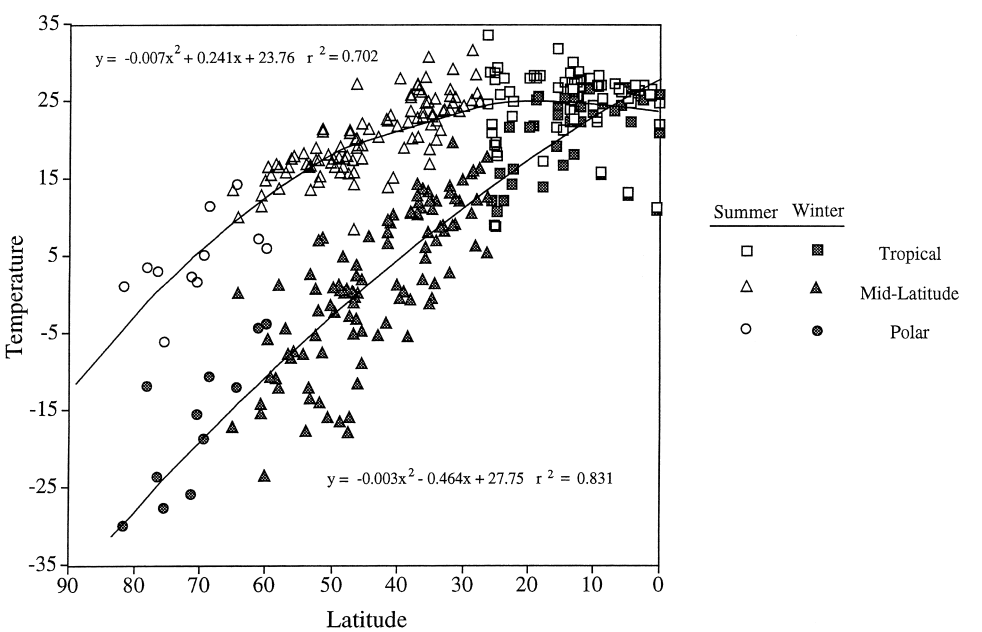

Fig. 1. Latitude versus temperature for summer and winter climate modes. Each point represents averages for an individual IAEA/WMO station. Trends for both modes are characterized by flat slopes in the tropics that become steeper with increasing latitude, and by similar correlation coefficients. Temperatures are uniformly higher and global temperature ranges are smaller under summer climate conditions.

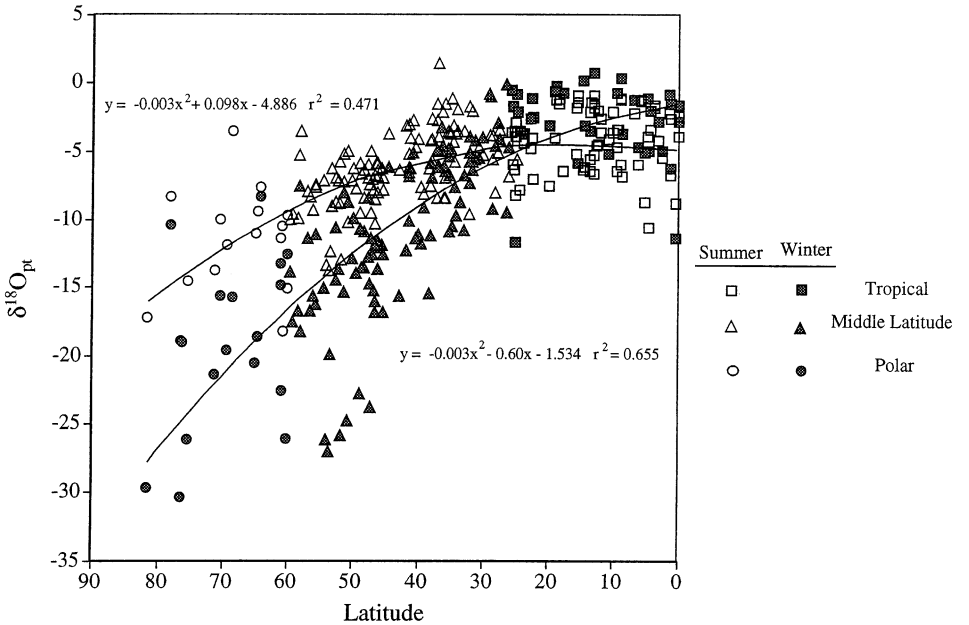

Fig. 2. Latitude versus $\delta^{18}O$ value of precipitation for summer and winter climate modes. Each point represents averages for an individual IAEA/WMO station. Trends are similar to those in Fig. 1 except for the crossover in trends for summer and winter climate modes, and the weaker correlation for summer relative to winter climate conditions. These features demonstrate the influence of air mass rainout and evapotranspiration on $\delta^{18}O_{pt}$ in the tropics and extra-tropics, respectively.

gradients in $\delta^{18}O_{pt}$ with increasing latitude are shallower for summer than for winter climate modes. The similarities in latitudinal temperature gradients emphasize the role of air mass cooling in forming condensate that preferentially incorporates ^{18}O, thus lowering the $\delta^{18}O_{pt}$ of subsequent precipitation. In contrast to behavior at higher latitudes, however, $\delta^{18}O_{pt}$ values in the tropics are *lower* in summer than they are in winter. The resulting inversion of $\delta^{18}O_{pt}$/latitude trends is a reflection of the *amount effect*, and is due to the greater amount of precipitation that falls in the tropics in summer relative to winter ([3], fig. 19). Lastly, the correlation between $\delta^{18}O_{pt}$ and latitude depends strongly on climate mode, with the summer correlation being worse than the winter correlation. Poorer correlations probably arise from the influence of local factors other than temperature on $\delta^{18}O_{pt}$, and will be discussed below.

The global relation between temperature and $\delta^{18}O_{pt}$ is expressed most clearly by comparing the two variables directly, as has been done for weighted $\delta^{18}O_{pt}$ and mean annual temperature in the past [1–3]. What is new in the plot shown in Fig. 3 is a view of this same relation as it exists for different climate modes, as represented by data for summer and winter seasons. Although not shown, the mean annual relation lies between, and parallels, those for summer and winter climate conditions. Three important aspects of this plot are (1) the relatively invariant slope of the $\delta^{18}O_{pt}$/temperature relations at mid- to high-latitudes regardless of climate mode, (2) the significant offset between $\delta^{18}O_{pt}$/temperature relations under summer and winter climatic conditions, and (3) the weaker correlation that exists under summer compared to winter conditions. The constant slope implies that any steepening or shallowing of gradients in the temperature/latitude trend outside of the tropics is effectively mirrored by similar modifications of gradients in the $\delta^{18}O_{pt}$/latitude relation. Thus the role of temperature change in controlling air mass condensation, and hence $\delta^{18}O_{pt}$ change on a global scale, is reemphasized. The offset between $\delta^{18}O_{pt}$/temperature relations, however, indicates that *absolute* $\delta^{18}O_{pt}$ values at each locality are determined by factors that are unique to a given climate mode. Lastly, $\delta^{18}O_{pt}$/temperature relations with dif-

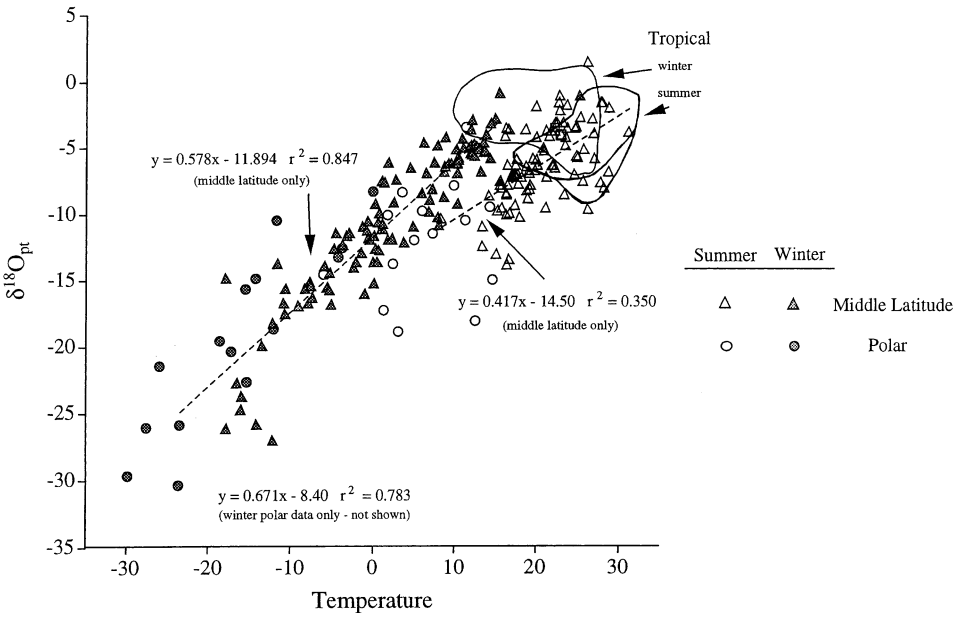

Fig. 3. $\delta^{18}O$ value of precipitation versus temperature for summer and winter climate modes. Each point represents averages for an individual IAEA/WMO station. Stations from tropical latitudes (individual data points not shown) and the six higher-latitude stations affected by the Asian monsoon are not included in calculating the slope and intercept of $\delta^{18}O_{pt}$/temperature relations. Relations for summer and winter climate modes have similar slopes, but are significantly offset due to the existence of different intercepts. As in Fig. 2, the correlation for summer climate mode is weaker than for winter due to non-temperature factors such as evapotranspiration, which may also account for the relatively high values for precipitation at polar stations.

ferent correlation coefficients indicate that factors other than temperature influence $\delta^{18}O_{pt}$ to varying degrees depending on climate mode.

4. Problems using a single $\delta^{18}O_{pt}$/temperature relation as a paleothermometer

In general, the relations between latitude, temperature, and $\delta^{18}O_{pt}$ (Figs. 1–3) indicate that surface temperature plays an overriding role in determining $\delta^{18}O_{pt}$ values on a global scale. Therefore any temporal change in climate mode that modifies latitudinal gradients in temperature will also modify global condensation patterns and hence $\delta^{18}O_{pt}$ at any given latitude (Fig. 2). In order to use this covariance as a quantitative paleothermometer, however, it is necessary to evaluate $\delta^{18}O_{pt}$/temperature relations that can vary systematically with climate mode, and the influence of factors other than temperature on $\delta^{18}O_{pt}$.

4.1. Offset of $\delta^{18}O_{pt}$/temperature relations with climate mode

4.1.1. Effects on estimating past temperatures and temperature change

One consequence of having climate-dependent relations between $\delta^{18}O_{pt}$ and temperature is that no single relation can be used unambiguously to infer absolute temperature *for all time periods* in the geological past. This restriction is particularly serious for 'Icehouse' and 'Greenhouse' time periods when the global distribution of heat and moisture, and hence intercepts of $\delta^{18}O_{pt}$/temperature relations, would likely have been very different from what they are at present (Fig. 3). For example, the mid-Cretaceous is characterized by warmer ocean temperatures and shallower latitudinal temperature gradients than at present [16], and it has been noted by previous authors [9] that the present-day weighted $\delta^{18}O_{pt}$/MAT relation is probably not valid for inferring temperatures at this time, especially in polar regions.

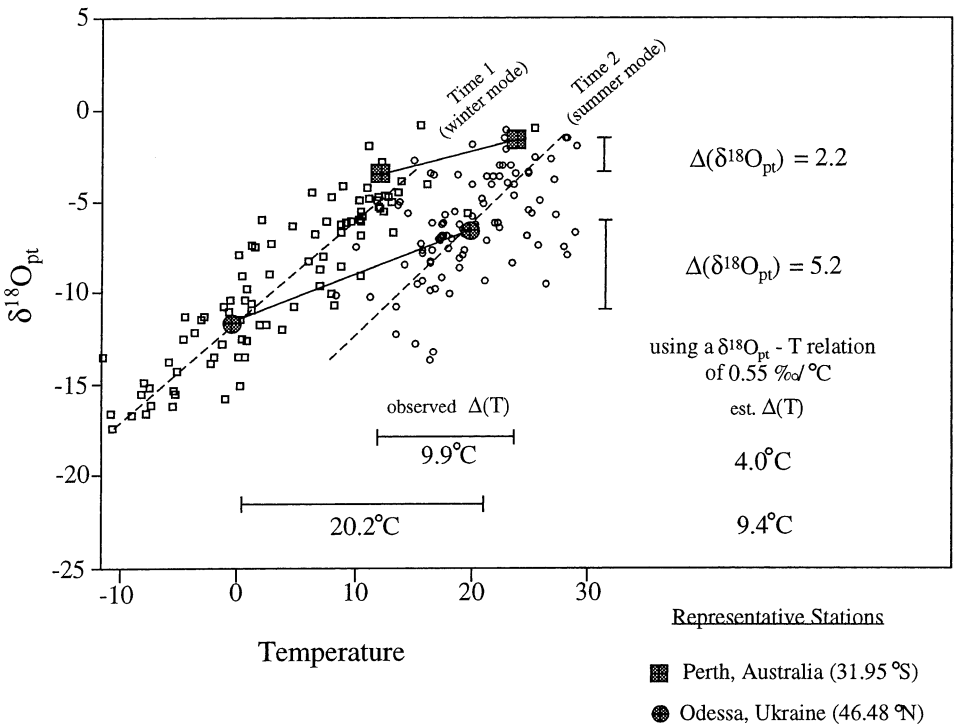

Fig. 4. Effect of two different $\delta^{18}O_{pt}$/temperature relations on paleotemperature estimates. Summer and winter data for precipitation at two representative middle-latitude localities (Perth, Australia, 31.95°S; Odessa, Ukraine, 46.48°N) are plotted along with the $\delta^{18}O_{pt}$/temperature relations for summer and winter climate modes. If a hypothetical temperature change over time takes place during a climate change from winter to summer conditions (or visa versa), and it is assumed that the slope of $\delta^{18}O_{pt}$/temperature relations do not change, the estimates of temperature change are almost half of those actually observed. This difference arises because the *temporal* $\delta^{18}O_{pt}$/temperature relations (solid lines) are shallower than *spatial* $\delta^{18}O_{pt}$/temperature relations (dashed lines).

Variable $\delta^{18}O_{pt}$/temperature relations also affect paleothermometry by making it difficult to quantify the amount of temperature change *over time* if there is a dramatic modification in climate mode. This difficulty arises because a comparison of data representing climate modes with offset $\delta^{18}O_{pt}$/temperature relations results in an underestimate of temperature change. To illustrate this point, temperature and $\delta^{18}O_{pt}$ data for two representative middle-latitude stations (Perth, Australia and Odessa, Ukraine) are plotted along with global $\delta^{18}O_{pt}$/temperature relations for summer and winter climate modes (Fig. 4). Proxy records of weighted $\delta^{18}O_{pt}$ covering a dramatic global change from cooler to warmer mean annual climate conditions at these localities would record changes of +2.2‰ and +5.2‰, respectively (vertical bars in Fig. 4). Using only the slope of the $\delta^{18}O_{pt}$/temperature relation, which has a relatively constant value of ~0.55‰/°C, these temporal changes in $\delta^{18}O_{pt}$ are interpreted to represent increases in temperature of 4.0 and 9.5°C, respectively. These estimates, however, are only about *half* of the 9.9 and 20.2°C changes in temperature that are actually observed at each locality (horizontal bars, Fig. 4). Similarly, estimates of temperature decrease made in the same manner will be too low.

The apparent underestimation of temperature change over time compared to temperature change over space using has $\delta^{18}O_{pt}$ has been observed at both seasonal [10,11] and geologic time scales [12], and it can be used to question the validity of the $\delta^{18}O_{pt}$ paleothermometer. It is clear from Fig. 4, however, that the reason seasonal temperature change is underestimated is that *temporal* $\delta^{18}O_{pt}$/temperature relations are shallower than *spatial* $\delta^{18}O_{pt}$/temperature relations. The two types of

relations are very different because temporal $\delta^{18}O_{pt}$/temperature relations are site-specific, being created by comparing data for different climate modes (solid lines in Fig. 4), while the spatial $\delta^{18}O_{pt}$/temperature relations represent global conditions for each specific climate mode (dashed lines, Fig. 4). A similar argument was presented by Boyle [13], who showed that ice core $\delta^{18}O_{pt}$ records from Greenland will underestimate glacial/interglacial temperature change relative to borehole thermometry records if an offset in $\delta^{18}O_{pt}$/temperature relations for the two periods is not taken into account. Lastly, it can be inferred from Fig. 4 that no matter what the offset in $\delta^{18}O_{pt}$/temperature relations over time, the extent to which temperature change is underestimated at a given latitude will remain relatively constant as long as the *slopes* of the $\delta^{18}O_{pt}$/temperature relations do not vary significantly.

4.1.2. Causes of offsets in $\delta^{18}O_{pt}$/temperature relations

Beyond discussing the effects of offset $\delta^{18}O_{pt}$/temperature relations on paleothermometry, it is important to understand why the offset occurs between summer and winter climate modes. A primary reason for the offset is the seasonal change in insolation that results in higher surface temperatures at all latitudes in the summer. The importance of temperature in controlling the relative position of $\delta^{18}O_{pt}$/temperature relations has been illustrated by using temperature-dependent Rayleigh equations to model progressive condensation from low to high latitudes [1,9,13]. A change in the initial condensation temperature will result in an offset in the position of global $\delta^{18}O_{pt}$/temperature relations so that it remains exponential in nature, but is shifted in the same direction as observed for data representing summer and winter climate modes.

A change in the atmospheric water vapor budget in the tropics can also result in an offset in $\delta^{18}O_{pt}$/temperature relations between climate modes. This parameter is important because the tropics are the ultimate source of much of the moisture that ultimately reaches higher latitudes. Therefore any difference in the amount or initial $\delta^{18}O$ value of moisture in tropical air masses will necessarily affect the nature of the $\delta^{18}O_{pt}$/temperature relation at higher latitudes. For example, the amount of water vapor in tropical air masses is different in glacial and non-glacial periods [17] and $\delta^{18}O_{pt}$ varies between summer and winter climate modes (Fig. 2). Both of these factors are tied to changes in precipitation/evaporation ratios, air mass rainout, etc. These aspects of the tropical water vapor budget are quite important because their effects on $\delta^{18}O_{pt}$ are not related directly to changes in surface temperature, but rather to changes in atmospheric circulation patterns and the intensity of convective cooling. As a result, offsets in $\delta^{18}O_{pt}$/temperature relations at higher latitudes can be modified by conditions in the tropics that are independent of temperature changes at the surface.

Lastly, a change in the $\delta^{18}O$ value of ocean water in the tropics can cause an offset in $\delta^{18}O_{pt}$/temperature relations because the initial $\delta^{18}O$ value of water vapor formed in tropical source areas is significantly controlled by the $\delta^{18}O$ of the tropical oceans. Although unlikely to be an important variable seasonally, $\delta^{18}O$ of the oceans have varied by at least $\pm$1–2‰ over geologic time scales.

4.2. Influence of factors other than temperature on local $\delta^{18}O_{pt}$ values

The second major problem in interpreting temporal records of $\delta^{18}O_{pt}$ are the factors other than temperature that influence $\delta^{18}O_{pt}$ on a local scale, and their relative impact on climate mode. In addition to the position of air mass boundaries mentioned above [7,8], there are several other factors whose effects are discernible in Figs. 2 and 3. For example, evaporation of water from the surface (i.e. large lakes [18] and near-shore ocean water) and the transpiration of moisture by plants affects local $\delta^{18}O_{pt}$ values by sending moisture back into overlying air masses [19–21]. This recycling of precipitation influences the isotopic and mass balances of overlying air masses, and thus modifies local $\delta^{18}O_{pt}$ values that would be appropriate to the closed-system condition inherent to idealized Rayleigh condensation. The result is poorer correlations between latitude, temperature, and $\delta^{18}O_{pt}$ that are observed during summer when higher temperatures and more plant growth increase rates of evaporation and transpiration, respectively (Figs. 2 and 3). In addition, systematically higher $\delta^{18}O_{pt}$ values for stations in polar latitudes (Fig. 3) are likely the result of evaporation from

the oceans near the low pressure bands at ~60° latitude that introduces local moisture with relatively high $\delta^{18}O$ values to overlying air masses moving in from lower latitudes. Although more common in the tropics, the *amount effect* can also influence $\delta^{18}O_{pt}$ values at higher latitudes, as is evidenced by the systematically lower $\delta^{18}O_{pt}$ values for stations in coastal China that are in the path of the Asian monsoon. Lastly, evaporation of precipitation as it falls to the surface shifts the remaining liquid water to higher $\delta^{18}O_{pt}$ values, and is a common phenomenon in arid regions. This factor accounts for very high $\delta^{18}O_{pt}$ values at warm, arid locations [5].

Focusing on the seasonal data, it is clear that the relative importance of these factors in influencing $\delta^{18}O_{pt}$ at a given locality depends on the climate mode. As already noted, $\delta^{18}O_{pt}$/temperature correlations vary with climate mode due to changes in evapotranspiration and, from Figs. 2 and 3, it can be seen that evaporation of precipitation and monsoonal air circulation do not affect $\delta^{18}O_{pt}$ values to the same degree under summer and winter climate conditions. The implication of these observations is that any temporal change in weighted average $\delta^{18}O_{pt}$ at a given locality may reflect a change in temperature, a change in the relative influence of other non-temperature factors, or a combination of effects. In the absence of outside information, it is thus impossible to make a completely unambiguous interpretation of a temporal record of $\delta^{18}O_{pt}$ for a single locality.

5. Reconstructing $\delta^{18}O_{pt}$/temperature relations over geologic time

The fact that the present-day relation between weighted average $\delta^{18}O_{pt}$ and mean annual temperature cannot be used to make quantitative estimates of temperature change over all of geologic time is unfortunate, but there are other ways in which paleoclimatic information can be obtained using appropriate records of $\delta^{18}O_{pt}$. The most basic method involves reconstructing global $\delta^{18}O_{pt}$/temperature relations for the time periods being investigated, for example with direct measurements of preserved waters or of proxy materials.

5.1. Empirical reconstructions

$\delta^{18}O_{pt}$/temperature relations can be reconstructed by comparing records of $\delta^{18}O_{pt}$ from at least two localities that cover a wide range of latitude in combination with independent estimates of temperature from one of those localities. A hypothetical illustration of how this sampling strategy works is presented in Fig. 5. Temporal records of past $\delta^{18}O_{pt}$ at localities A and B are used to reconstruct latitudinal gradients in $\delta^{18}O_{pt}$ for time periods 1 and 2 that are characterized by a cooler and a warmer climate mode, respectively (Fig. 5, panel 1). Using these records, and assuming that the slopes of global $\delta^{18}O_{pt}$/temperature relations have relatively constant values of ~0.55‰/°C regardless of climate mode (Fig. 3), then it is possible to reconstruct global $\delta^{18}O_{pt}$/temperature relations for time periods 1 and 2 if an independent estimate of temperature is available from one of the localities. These temperatures can be inferred from geological, biological, and geochemical evidence at a given latitude. For example, terrestrial floral and faunal reconstructions or the $\delta^{18}O$ of planktonic foraminifera from latitudinally-equivalent marine sediments, could be used to anchor the position of the $\delta^{18}O$ data (Fig. 5, panel 2).

An obvious challenge lies in bringing together temporal records of $\delta^{18}O_{pt}$ from a wide range of latitudes. The relative difficulty of making such a comparison will depend on the proxy for $\delta^{18}O_{pt}$ that is being used, with certain materials like soil carbonate being less common over time and space than materials like biogenic apatite that is found in animal fossils. Comparing records of $\delta^{18}O_{pt}$ from different but related localities is profitable because it has the additional and very important advantage of reducing ambiguities otherwise associated with trying to interpret a temporal record of weighted $\delta^{18}O_{pt}$ values from a single locality. As mentioned above, these ambiguities stem from the possible influence of factors other than temperature on $\delta^{18}O_{pt}$ at any given place. By comparing $\delta^{18}O_{pt}$ records from a number of sites, however, the scale of investigation is changed from a site-specific scale where it may be difficult to distinguish the role of factors such as air mass boundaries and evapotranspiration on $\delta^{18}O_{pt}$, to a global scale where their effects are more likely to

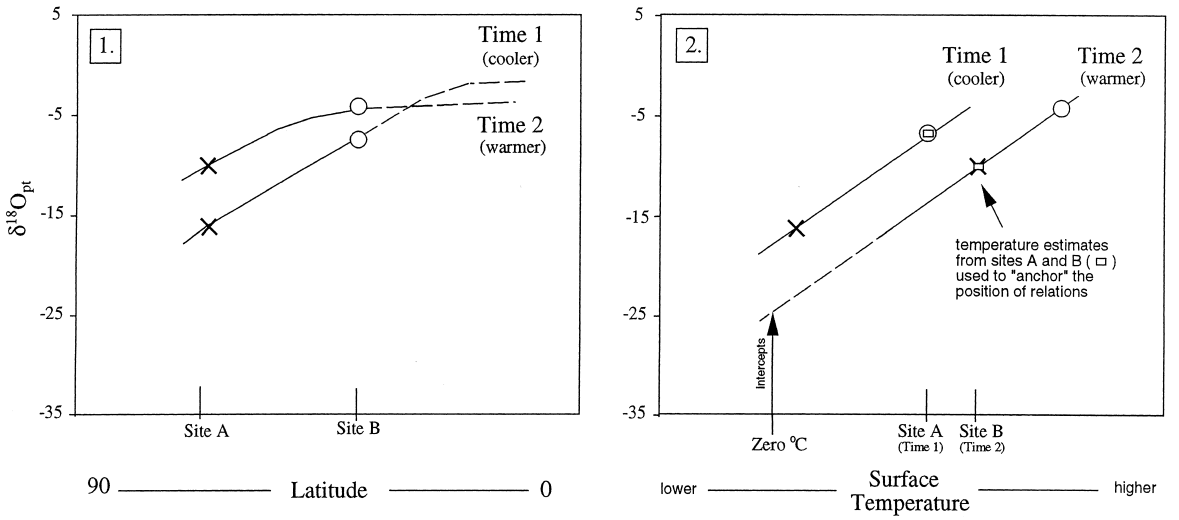

Fig. 5. Comparing $\delta^{18}O_{pt}$ records from a wide range of latitudes allows reconstructions to be made of $\delta^{18}O_{pt}$/temperature relations. In panel 1, weighted $\delta^{18}O_{pt}$ values from two different times and two different localities (sites A and B) are plotted versus paleolatitude. In this manner $\delta^{18}O_{pt}$/latitude gradients can be reconstructed for times 1 and 2 when global climate was significantly different. Using independent temperature estimates from the latitudes of sites A and B, and assuming that the $\delta^{18}O_{pt}$/temperature relation has a constant slope of ~0.55‰/°C, it is possible to reconstruct $\delta^{18}O_{pt}$/temperature relations and their intercepts for times 1 and 2 (panel 2).

stand out as anomalies in a global pattern, and can be interpreted as such.

The major drawback to this empirical method of reconstructing $\delta^{18}O_{pt}$/temperature relations is that it relies on 'outside' estimates of temperature from the very same kinds of proxy records the relations are aimed to replace. If these independent temperature estimates themselves are poorly quantified, as is the case for estimates based on sedimentology, then the usefulness of reconstructed $\delta^{18}O_{pt}$/temperature relations will be diminished.

5.2. Model reconstructions

Another method of reconstructing $\delta^{18}O_{pt}$/temperature relations relies on theoretical calculations of global condensation that assume Rayleigh conditions [1,9,14] rather than on empirical data, but it is not without problems of its own. As in the case of empirical reconstructions, the use of model equations requires some knowledge of surface temperatures, in particular tropical temperatures, for each time period of interest [14]. In addition, it is necessary to have an estimate of the $\delta^{18}O$ value of tropical ocean water in order to get the most accurate results using the theoretical models. More importantly, it has been noted that Rayleigh equations are only an approximation of the complex global condensation process [5], and thus may not be completely accurate in any case. For example, the exponential Rayleigh equations cannot reproduce the global $\delta^{18}O_{pt}$/temperature trends that form as the result of decoupling between atmospheric processes occurring in tropical and extra-tropical regions (Fig. 3).

6. Additional ways of using estimates of $\delta^{18}O_{pt}$ to study climate in the past

In the above discussion we reviewed the difficulties involved in using $\delta^{18}O_{pt}$/temperature relations as quantitative paleothermometers over geologic time, and noted that the approach to resolving these problems will depend on the paleoenvironmental and isotopic data available for a given time period or region. There are, however, alternative ways in which paleoclimatological information can be obtained using oxygen isotope data that do not rely on reconstructing $\delta^{18}O_{pt}$/temperature relations in the past.

6.1. Direct estimates of temperature using biogenic apatite as a proxy for $\delta^{18}O_{pt}$

One way to estimate temperature without relying on $\delta^{18}O_{pt}$/temperature relations is to utilize equations that describe oxygen isotope fractionation between water (precipitation) and different mineral phases that form in equilibrium with it. A novel example of this approach involves the measurement of $\delta^{18}O$ values of a *single* substance that forms under *different* conditions in *different* surficial environments [22]. In particular, $\delta^{18}O$ of apatite coming from mammalian fossils can be used to determine the $\delta^{18}O$ of ingested water (precipitation) because the apatite forms at the constant body temperature of the animal (~37°C). Combining this information with $\delta^{18}O$ values of associated fish fossils and using the phosphate paleothermometer of Longinelli and Nuti [23], it is then possible to estimate the temperature of river water, which mirrors that of air temperature. Oxygen isotope analyses of mammalian tooth enamel and fresh water fish scales were recently used in this manner to infer temperature change during the early Paleogene [24], and the widespread occurrence of biogenic apatite over time and space may make this sampling strategy a reasonable alternative to reconstructing $\delta^{18}O_{pt}$/temperature relations.

6.2. Using $\delta^{18}O_{pt}$ to validate GCM predictions

A quite different approach to using records of $\delta^{18}O_{pt}$ to study terrestrial paleoclimatology does not rely on $\delta^{18}O_{pt}$ to estimate temperature, or any other climate variable. Instead, records of $\delta^{18}O_{pt}$ are used to test predictions of global climate models (GCM) which are in turn used to elucidate the nature of climate change (for a review see [25]). The goal of integrating oxygen isotope systematics with GCMs is to predict the spatial distribution of $\delta^{18}O_{pt}$ in the past by accounting for oxygen isotope fractionations that accompany phase changes that take place as water 'moves' through the hydrologic cycle during a climate simulation. A comparison of the predicted distribution with the actual distribution obtained from records of $\delta^{18}O_{pt}$ then provides a much-needed check on the ability of GCMs to replicate complex changes in climate over geologic time. This method is appealing because, in contrast to focusing on a single variable such as temperature, GCM predictions have the potential to provide a much more complete picture of how several climatic variables like vegetation cover, ocean/atmospheric circulation patterns, pCO_2, heat transfer, the hydrologic cycle, etc., interact to produce a change in climate.

Attempts to reproduce modern patterns in $\delta^{18}O_{pt}$ using GCM model predictions have been relatively successful indicating that the potential exists for combined GCM-isotope investigations of terrestrial paleoclimate [26,27]. More recent efforts have focused on comparing model predictions and proxy records of $\delta^{18}O_{pt}$ for the last glacial maximum [28,29]. Continued study of these well-characterized time periods should help refine the model-isotope approach to studying terrestrial climate change over a much broader range of geologic time.

7. Conclusions

Separating the global data base of temperature and isotopic measurements into climate modes defined by summer and winter climate conditions, provides a simple model for understanding how global relations between $\delta^{18}O_{pt}$ and temperature can be offset relative to one another as a result of differences in temperature and air mass rainout in the tropics. It is not always possible to use the well known weighted $\delta^{18}O_{pt}$/MAT relation to make accurate interpretations of a temporal record of $\delta^{18}O_{pt}$ values, especially if climate mode in the geologic past was radically different from that at present, or if climate change over time was extreme. While there is a strong relation globally between $\delta^{18}O_{pt}$ and temperature regardless of the source area and transport history of air masses, there are a number of factors other than temperature that can mask the $\delta^{18}O_{pt}$/temperature relation on a local/regional scale. The effect of these factors can vary depending on climate mode, making the interpretation even more ambiguous.

At present, there are three ways to circumvent problems associated with the $\delta^{18}O_{pt}$ paleothermometer in terrestrial environments. One may compare $\delta^{18}O_{pt}$ records from localities that cover a wide range of latitudes with independent estimates of temperature to reconstruct global $\delta^{18}O_{pt}$/temperature rela-

tions for different time periods in the past. Under certain favorable conditions, it may also be possible to estimate temperature using records of $\delta^{18}O_{pt}$ without relying on any $\delta^{18}O_{pt}$/temperature relation. The most profitable use of $\delta^{18}O_{pt}$ records may lie in their ability to test the accuracy of climate-change predictions produced using global climate models. ***[CL]***

References

[1] W. Dansgaard, Stable isotopes in precipitation, Tellus 16 (1964) 436–468.

[2] Y. Yurtsever, J.R. Gat, Atmospheric waters, in: J.R. Gat, R. Gonfiantini (Eds.), Stable Isotope Hydrology — Deuterium and Oxygen-18 in the Water Cycle, IAEA, Int. Atomic Energy Agency Tech. Rept. Ser., 1981, pp. 103–142.

[3] K. Rozanski, L. Araguás-Araguás, R. Gonfiantini, Isotopic patterns in modern global precipitation, in: P.K. Swart, K.C. Lohmann, J. McKenzie, S. Savin (Eds.), Climate Change in Continental Climate Records, Am. Geophys. Union, Geophys. Monogr. 78 (1993) 1–36.

[4] H. Craig, L.I. Gordon, Deuterium and oxygen-18 variations in the ocean and the marine atmosphere, in: E. Tongiorgi (Ed.), Proceedings of a conference on stable isotopes in oceanographic studies and paleotemperatures, Consiglio Nazionale della Richerche, Pisa, 1965, pp. 9–130.

[5] J.R. Gat, Oxygen and hydrogen isotopes in the hydrologic cycle, Annu. Rev. Earth Planet. Sci. 24 (1996) 225–262.

[6] P.K. Swart, K.C. Lohmann, J. McKenzie, S. Savin (Eds.), Climate Change in Continental Climate Records, Am. Geophys. Union, Geophys. Monogr. 78 (1993).

[7] T.W.D. Edwards, B.B. Wolfe, G.M. MacDonald, Influence of changing atmospheric circulation on precipitation δ^{18}O-temperature relations in Canada during the Holocene, Quat. Res. 46 (1996) 211–218.

[8] R. Amundson, O. Chadwick, C. Kendall, Y. Wang, M. DeNiro, Isotopic evidence for shifts in atmospheric circulation patterns during the late Quaternary in mid-North America, Geology 24 (1996) 23–26.

[9] R.T. Gregory, C.B. Douthitt, I.R. Duddy, P.V. Rich, P.H. Rich, Oxygen isotopic composition of carbonate concretions from the lower Cretaceous of Victoria, Australia: implications for the evolution of meteoric waters of the Australian continent in a paleopolar environment, Earth Planet. Sci. Lett. 92 (1989) 27–42.

[10] J.R. Lawrence, J.W.C. White, The elusive climate signal in the isotopic composition of precipitation, in: H.P. Taylor, J.R. O'Neil, I.R. Kaplan (Eds.), Stable Isotope Geochemistry: A Tribute to Samuel Epstein, The Geochemical Society, Special Publication, 1991, pp. 169–185.

[11] K. Rozanski, L. Araguás-Araguás, R. Gonfiantini, Relation between long-term trends of oxygen-18 isotope composition of precipitation and climate, Science 258 (1992) 981–985.

[12] K.M. Cuffey, R.B. Alley, M. Stuiver, E.D. Waddington, R.W. Saltus, Large arctic temperature change at the Wisconson–Holocene glacial transition, Science 270 (1995) 455–458.

[13] E.A. Boyle, Cool tropical temperatures shift the global δ^{18}O–*T* relationship, Geophys. Res. Lett. 24 (1997) 273–276.

[14] IAEA/WMO, Global Network for Isotopes in Precipitation — the GNIP Database, Release 1, URL: http://www.iaea.org/programs/ri/gnip/gnipmain.htm, 1997.

[15] C. Sonntag, K. Rozanski, K.O. Munnich, H. Jacob, Variations of deuterium and oxygen-18 in continental precipitation and groundwater and their causes, in: A. Street-Perot et al. (Eds.), Variations in the Global Water Budget, D. Reidel, Dordrecht, 1983, pp. 107–124.

[16] B.T. Huber, D.A. Hodell, C.P. Hamilton, Middle–Late Cretaceous climate of the southern high latitudes: Stable isotopic evidence for minimal equator-to-pole thermal gradients, Geol. Soc. Am. Bull. 107 (1995) 1164–1191.

[17] W. Broecker, Mountain glaciers: Recorders of atmospheric water vapor content?, Global Biogeochem. Cycles 11 (1997) 589–597.

[18] M.V. Machavaram, R.V. Krishnamurthy, Earth surface evaporative process: A case study from the Great Lakes region of the United States based on deuterium excess in precipitation, Geochim. Cosmochim. Acta 59 (1995) 4279–4283.

[19] E. Salati, A. Dall'ollio, E. Matsui, J. Gat, Recycling of water in the Amazon Basin, an isotopic study, Water Resources Res. 15 (1979) 1250–1258.

[20] H. Jacob, C. Sonntag, An 8-year record of the seasonal variation of ^{2}H and ^{18}O in atmospheric water vapor and precipitation at Heidelberg, Germany, Tellus 43B (1991) 291–300.

[21] R.D. Koster, D.P.d. Valpine, J. Jouzel, Continental water recycling and $H_2{}^{18}O$ concentrations, Geophys. Res. Lett. 20 (1993) 2215–2218.

[22] Y. Kolodny, B. Luz, O. Navon, Oxygen isotope variations in phosphate of biogenic apatite, I: fish bone apatite, Earth Planet. Sci. Lett. 64 (1983) 398–404.

[23] A. Longinelli, S. Nuti, Revised phosphate–water isotopic temperature scale, Earth Planet. Sci. Lett. 19 (1973) 373–376.

[24] H. Fricke, W. Clyde, J. O'Neil, P. Gingerich, Evidence for rapid climate change in North America during the latest Paleocene thermal maximum: oxygen isotope composition of biogenic phosphate from the Bighorn Basin (Wyoming), Earth Planet. Sci. Lett. 160 (1998) 193–208.

[25] J. Jouzel et al., Validity of the temperature reconstruction from water isotopes in ice cores, J. Geophys. Res. 102 (1997) 26471–26487.

[26] S. Joussaume, J. Jouzel, R. Sadourny, A general circulation model of water isotope cycles in the atmosphere, Nature 311 (1984) 24–29.

[27] J. Jouzel, R. Koster, R. Suozzo, G. Russell, J. White, W.

Broecker, Simulations of the HDO and $H_2{}^{18}O$ atmospheric cycles using the NASA GISS general circulation model: Sensitivity experiments for present-day conditions, J. Geophys. Res. 96 (1991) 7495–7507.

[28] S. Joussaume, J. Jouzel, Paleoclimatic tracers: An investigation using an atmospheric general circulation model under ice age conditions 2. Water isotopes, J. Geophys. Res. 98 (1993) 2807–2830.

[29] J. Jouzel, R.D. Koster, R.J. Suozzo, G.L. Russell, Stable water isotope behaviour during the last glacial maximum: A general circulation model analysis, J. Geophys. Res. 99 (1994) 25791–25801.